

Raman scattering by magnetic excitations and phonons in diluted magnetic structures formed by self-organized quantum disks of CdZn(Mn)Se in a Zn(Mn)Se matrix

I. I. Reshina,* S. V. Ivanov, D. N. Mirlin, and A. A. Toropov
Ioffe Physico-Technical Institute, 194021 St. Petersburg, Russia

A. Waag
Abteilung Halbleiterphysik, Universität Ulm, 89081 Ulm, Germany

G. Landwehr
Physikalisches Institut der Universität Würzburg, D-97074 Würzburg, Germany

(Received 21 December 2000; revised manuscript received 12 April 2001; published 13 June 2001)

Photoluminescence and resonant Raman scattering by magnetic excitations and optical phonons were studied in diluted magnetic structures that consisted of nominally two monolayer depositions of CdSe between ZnSe barriers. Mn was incorporated either into the CdSe layers or into the barriers. Self-organized quantum islands of composition CdZnSe are formed in the “well” layers during growth. Luminescence bands of excitons localized at the islands showed under applied magnetic fields strong effects of s,p - d exchange interaction of band carriers with Mn^{2+} ions. Different types of magnetic excitation were observed in resonant Raman scattering spectra, such as spin-flip scattering of the donor-bound magnetic polarons at the CdZnSe islands, Raman transitions between ground and first excited states of antiferromagnetically coupled nearest neighbor Mn^{2+} ions, and collective multiple spin-flip Raman scattering within a Zeeman split Mn^{2+} ground state. The Raman spectra of optical phonons were studied under resonance and off-resonance excitation.

DOI: 10.1103/PhysRevB.64.035303

PACS number(s): 78.30.Fs, 75.75.+a

I. INTRODUCTION

Great attention has been paid recently to structures with nominally mono- and submonolayer depositions of CdSe in a ZnSe matrix, grown by molecular beam epitaxy (MBE), due to their feasibility as active media in optoelectronic devices in the blue-green spectral region.^{1,2} Such structures are also of fundamental physical interest because flat CdZnSe islands with 10–100 nm lateral dimension (actually quantum disks) are formed during the growth of CdSe layers below critical thickness, as was shown by transmission electron microscopy² (TEM) and high resolution TEM images of the samples.^{3–5} It was demonstrated by resonant Raman scattering that at low temperatures excitons are localized at these islands and mediate strong resonance scattering by LO phonons.⁶ The zero-dimensional nature of excitons in such CdSe/ZnSe structures was also confirmed by observation of single-exciton lines in spatially resolved photoluminescence,^{5,7} micro-Raman,⁸ and cathodoluminescence⁹ experiments. Another clear indication of the strong three-dimensional confinement of excitons is a long lifetime up to 550 ps, independent of temperature up to 130 K, as reported for the single-exciton lines.⁵

For many years diluted magnetic semiconductors (DMS's) such as CdMnTe or CdMnSe have been the subject of fundamental studies because of the large exchange interactions between the charge carriers and the magnetic ions.¹⁰ Recently, the interest in DMS structures has been renewed due to the growing attention to semiconductor spin devices.¹¹ Especially useful for spin-memory and spin-injection devices might be DMS nanostructures with three-dimensional electron confinement, because complete quantization of the energy spectrum substantially increases the spin relaxation

time.¹² Therefore, fabrication of such samples and studies of the spin-flip processes and magnetic excitations are of considerable importance.

Raman studies have been reported on various DMS superlattice¹³ and quantum well structures,^{14–16} where excitons act as intermediate states in the scattering processes. However, to our knowledge there have been no data reported on Raman studies of DMS nanostructures with well established zero-dimensional nature of excitons. In this paper we report on fabrication and detailed Raman studies of Cd(Mn)Se/Zn(Mn)Se DMS samples. By analogy with the well-known CdSe/ZnSe samples we anticipate formation of quantum disk structures and focus on the resonant Raman scattering by phonons and magnetic excitations of various kinds.

II. SAMPLES AND EXPERIMENTAL SETUP

The Cd(Mn)Se/Zn(Mn)Se DMS samples were grown by MBE pseudomorphically on GaAs (001) substrates at $T = 280^\circ\text{C}$. The nominal thickness of Cd(Mn)Se insertions in all the samples was around 2 monolayers with 10% accuracy. As shown previously,^{1,6} this nominal thickness is pertinent to formation of well-defined ZnCdSe flat islands. Mn was incorporated either into the CdSe layer or into the ZnSe barriers. An additional carrier confinement was achieved by wider band gap $Zn_{0.97}Be_{0.03}Se$ layers on both sides of the 10 nm Zn(Mn)Se barriers. Five samples of three types were studied, as shown schematically in Fig. 1. In type A Mn was introduced into the CdSe layer, whereas in type B Mn was introduced into the ZnSe barriers. [In types A and B one could not exclude the presence of Mn in the adjacent layers—barriers (type A) or “wells” (type B)—due to inter-

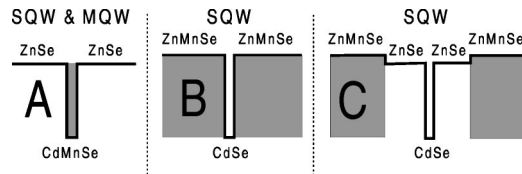


FIG. 1. Schematic representation of the samples.

diffusion.] In type C Mn was incorporated into the barrier, but a nonmagnetic ZnSe spacer layer of 1.6 nm width was inserted on both sides of the CdSe layer. The nominal Mn content in all samples is given in Table I. The samples were not intentionally doped, but “as grown” CdSe and ZnSe samples are known to be *n* type. Average concentration of Cd in the islands was approximately 0.2, as found from Raman scattering by LO phonons.

The experiments were carried out in a He cryostat with a superconducting coil which provided magnetic fields up to 6.5 T. The samples could be immersed either in pumped liquid He ($T=1.7$ K) or in He vapor ($T\sim 6$ K). In the latter case the temperature could be increased with the aid of a small electric oven. The Raman and luminescence spectra were recorded in the backscattering Faraday or Voigt geometry by Yobin Ivon U-1000 (linear dispersion 0.24 nm/cm) or DFS-24 (linear dispersion 0.5 nm/cm) spectrometers with double-grating monochromators and photon counting electronics. The samples were excited by the blue-green lines of a cw Ar⁺ laser.

III. EXPERIMENTAL RESULTS AND DISCUSSION

A. Luminescence

Under excitation below the ZnSe barrier band gap with 2.6 eV energy photons, broad luminescence bands (20–80 meV) in the region of 2.5 eV were observed related to heavy hole excitons localized in the CdZnSe islands. The exciton luminescence in Faraday configuration showed strong dependence on the applied magnetic field B . The luminescence intensity increased appreciably with increasing B , the band broadened from the low energy side,¹⁷ and the peak position shifted to lower energies. The shift of luminescence bands in Faraday geometry as a function of applied magnetic field is shown in Fig. 2. Large shifts indicate strong splitting of the conduction and valence bands caused by the *s,p-d* exchange interaction between *d* electrons of Mn²⁺ ions and the band carriers. We attribute the observed luminescence bands to $| -1/2, +3/2 \rangle$ excitons localized in the quantum disks. Under magnetic field the luminescence bands were strongly circularly polarized with the degree of polarization $\rho_c=0.96$ at $B=6$ T. For sample C, the exciton band shifted only by about 10 meV at a field $B=6$ T and $\rho_c=0.7$ was measured.

TABLE I. Content of Mn in the samples.

Type A		Type B		Type C
A1	A2 ^a	B1	B2	C
0.15	0.07	0.11	<0.01	0.11

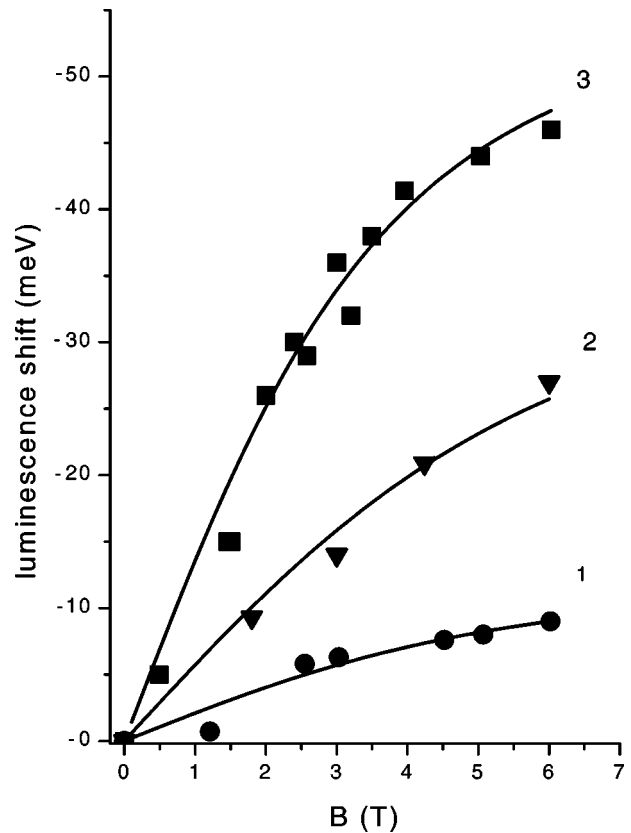
^aFive insertions of CdSe.

FIG. 2. Luminescence shift as a function of magnetic field for different samples in Faraday geometry. Samples: 1, C; 2, A2; 3, B1. Solid lines are fits to the experimental data in the framework of a molecular field model.

This is not surprising considering the decreased overlap of the exciton wave function with the Mn²⁺ ions due to the nonmagnetic spacer.

In the Voigt geometry the shift of the peak position to lower energy was much smaller in all samples. This is obviously due to strong magnetic anisotropy of the valence band. It is known that for narrow or strained quantum wells in the Voigt geometry the states of heavy holes $|3/2, +3/2\rangle$ and $|3/2, -3/2\rangle$ split very slightly in a magnetic field or are even degenerate.^{18,19}

B. Spin-flip Raman scattering of the donor-bound electrons

The luminescence bands of sample C at $B=6$ T in Faraday geometry under nonresonant (2.6 eV) and resonant (2.495 eV) excitation are shown in Fig. 3. As is seen from Fig. 3, a line appears in the emission spectrum under resonant excitation. Its position depends strongly on the magnetic field, as is seen in Fig. 4. Under the condition of sharp resonance with the excitons localized in the quantum disks, this line was observed in both Stokes and anti-Stokes regions in the $\sigma_-\sigma_+$ and $\sigma_+\sigma_-$ polarizations, respectively, Fig. 5. Thus we conclude that it is a Raman line and assign it to a spin-flip transition of a donor-bound electron in CdZnSe islands between $m=-1/2$ and $m=1/2$ states split by the exchange interaction with *d* electrons of Mn²⁺ ions in the ZnSe barriers. We think that this line is related to the donor-bound

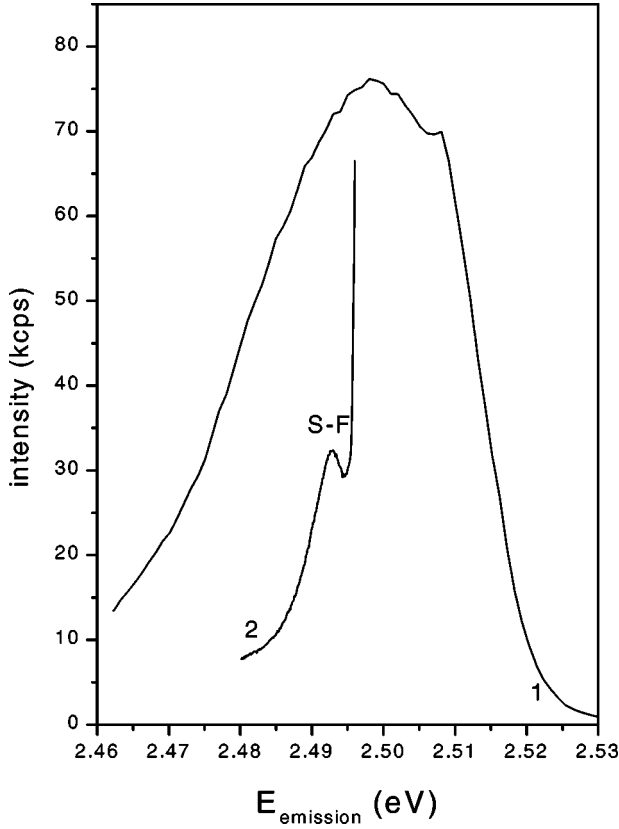


FIG. 3. Luminescence under off-resonance (1) and resonance (2) excitation. Faraday geometry. Sample C, $B=6$ T. Line 1, $E_{exc}=2.6$ eV; line 2, $E_{exc}=2.495$ eV. S-F is the spin-flip line.

electrons, rather than to the photoexcited ones, because the ratio of its intensity to the incident laser power does not increase with increasing laser power.

The dependence of the spin-flip energy ΔE on B is shown in Fig. 6 at $T=1.7$ K for the samples B2 and C. A much smaller ΔE was measured at $T=10$ K, as is shown for $B=6$ T. The ΔE dependence on B was analyzed according to the expression²⁰

$$\Delta E = x_{eff} \alpha N_0 \langle S_z^{Mn} \rangle + g^* \mu_B B \quad (1)$$

(solid lines in Fig. 6) where in our case

$$x_{eff} = \int \varphi^2(\vec{r}) \bar{x}(\vec{r}) d\vec{r} \quad (2)$$

is the effective content of the Mn^{2+} ions that take part in the exchange interaction with the donor-bound electrons. φ is the envelope wave function of the donor-bound electron, α is the exchange interaction constant between localized spins of Mn^{2+} ions and that of the electrons, N_0 is the number of cations per unit cell, g^* is the Landé factor of the electron in the “well,” μ_B is the Bohr magneton, and $\langle S_z^{Mn} \rangle$ is the thermal average of the Mn spin projection along \mathbf{B} and is given by the modified Brillouin function B_S for $S=5/2$,

$$\langle S_z^{Mn} \rangle = (5/2) B_{5/2} [S g \mu_B B / k_B (T + T_{AF})], \quad (3)$$

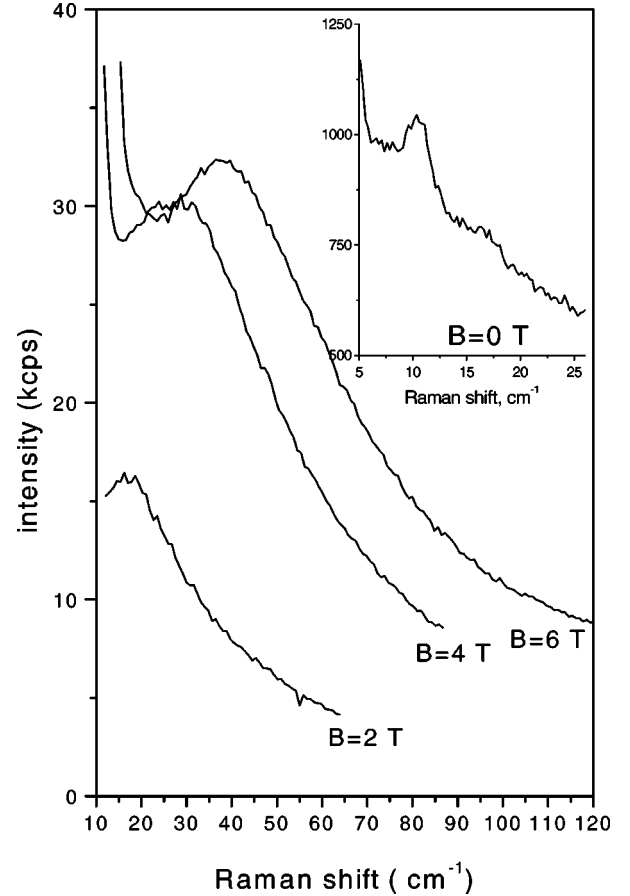


FIG. 4. Spin-flip Raman lines of donor-bound electrons at different magnetic fields. Faraday geometry, sample C, $E_{exc}=2.495$ eV, $T=1.7$ K. In the inset, S-F line at $B=0$ T.

where $g=2$ for electrons of the inner Mn shell. The actual Mn content \bar{x} is smaller than the nominal content x due to antiferromagnetic pairing of Mn^{2+} ions. The parameter T_{AF} also reflects Mn^{2+} pairing.

Equations (1) and (3) have two adjustable parameters x_{eff} and T_{AF} . We obtained from the fit $x_{eff}=0.007$ and $T+T_{AF}=6$ K for the sample C, and $x_{eff}=0.004$ and $T+T_{AF}=4$ K for the sample B2. Probably the sample C was a little heated by focused laser light, although the incident power was about $5-10$ W/cm².

Note that the value of x_{eff} for the sample C was found to be an order of magnitude less than the actual concentration of Mn in the barriers, in general agreement with the theoretical estimations performed within the envelope function approximation. A very close value of x_{eff} was found from fitting the luminescence peak position on B . This effective value of Mn content can be regarded as a characterization of the excitonic wave function (or the donor-bound electron wave function) localization in the z direction. In the region where the fitting curve depends linearly on B , an effective g factor was estimated as $g_{eff} \sim 9$ for the sample C (as compared with $g^*=0.52$ and 1.1 for conduction band electrons in bulk CdSe and ZnSe, respectively).

One can see in Fig. 4 that the spin-flip line (S-F) broadens with increase of the magnetic field, i.e., Raman shift. It is

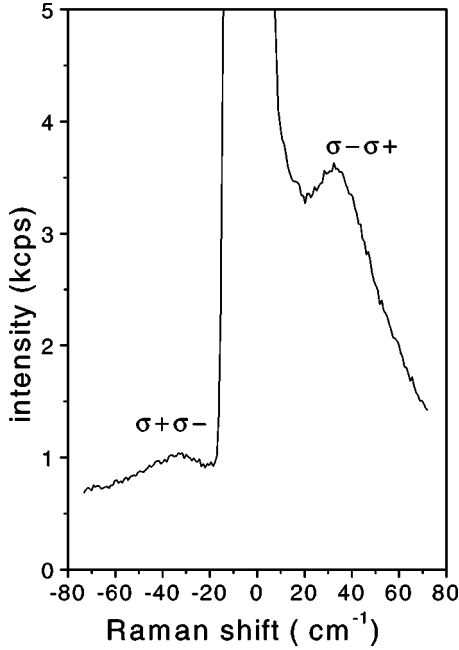


FIG. 5. Stokes and anti-Stokes spin-flip Raman scattering of donor-bound electrons. Faraday geometry, sample C, $B=4.4$ T, $E_{exc}=2.495$ eV, $T=1.7$ K.

difficult to evaluate precisely the full width at half maximum (FWHM) of the S-F line because of the strong sloping luminescence background. We estimate the FWHM at $B=0$ T as 3 cm^{-1} , at $B=2$ T as 15 cm^{-1} , and at $B=6$ T as 29 cm^{-1} (see Fig. 7). The FWHM almost saturates at $B>3$ T. An increase of the FWHM with increasing magnetic field (or Raman shift) was observed for bulk CdMnTe epilayers.²¹ In our case the dependence on B is much stronger. This dependence can be clarified by the following consideration. The effective g factor can be displayed as

$$g_{eff} = \bar{g} \pm \delta g, \quad (4)$$

where \bar{g} is the average g factor, which determines the position of the spin-flip Raman line, and δg determines its FWHM.

Thus, the FWHM is given by $2\delta g B$, i.e., it increases with increasing B . δg varies for different CdZnSe islands due to Cd concentration and quantum confinement fluctuations in various islands. Both factors might change the overlap with the Mn^{2+} ions on one hand and produce different kinetic exchange contribution for electrons on the other hand.²²

It was shown in Ref. 22 that the exchange constant α might change when the kinetic exchange contribution for electrons becomes possible by the admixture of the valence band states with p -like symmetry in the electron wave function. Hence, the kinetic exchange contribution would depend on the quantum confinement.

The spin-flip line was also present in samples C, B2, and A2 at $B=0$ T, as is seen in Fig. 6, in the inset to Fig. 4, and in Fig. 8. The nonzero Raman shift at $B=0$ T is indicative of bound magnetic polaron formation.^{23,24}

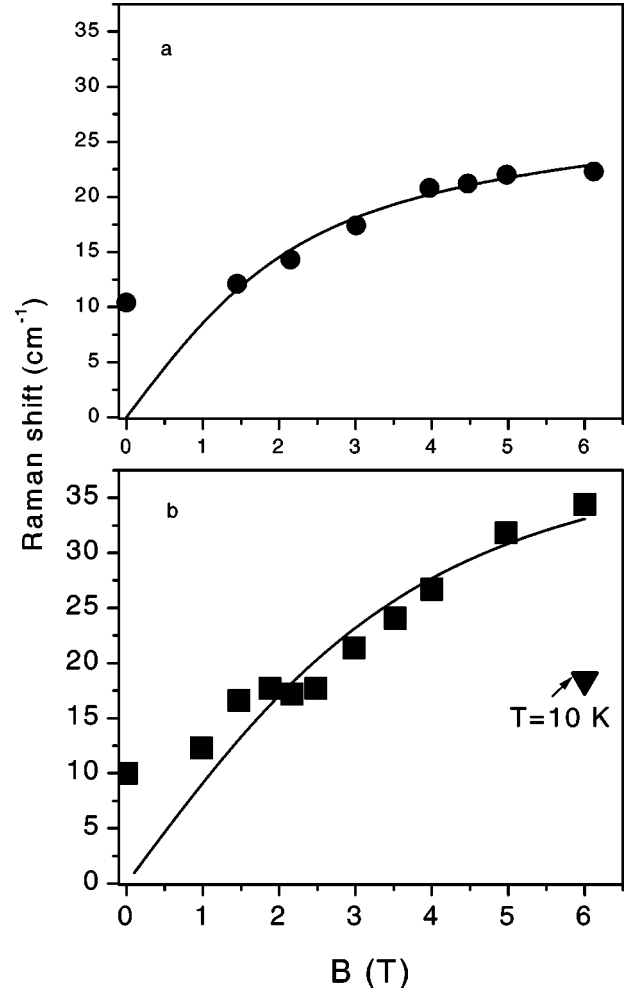


FIG. 6. Raman shift of the spin-flip line versus B . Faraday geometry. (a) Sample B2, $E_{exc}=2.54$ eV. (b) Sample C, $E_{exc}=2.495$ eV, $T=1.7$ K. Solid lines are fits according to Eq. (1) and Eq. (3).

In samples A1 and B1 we could not observe spin-flip Raman lines in Faraday geometry due probably to unfavorable resonance conditions. In the Voigt geometry we observed very broad and weak spin-flip lines with large shifts under high magnetic fields. However, at low fields and at $B=0$ the low energy side of the line was masked by Rayleigh scattered light, which prevented accurate determination of the peak position. We estimate the zero-field Raman shift in the sample B1 as 19 ± 5 cm^{-1} .

C. Spin-flip transition due to antiferromagnetically coupled Mn pairs

At $B=0$ T along with the bound magnetic polaron line another weak Raman line was observed under resonant excitation for sample C at ~ 17 cm^{-1} . The same line was detected with greater intensity in the samples A and B1. This line is shown in Fig. 8 for sample A2 with five insertions of CdSe separated by ZnSe barriers. This line does not obey particular polarization selection rules and its position does not depend on the magnetic field up to $B=6.5$ T. We at-

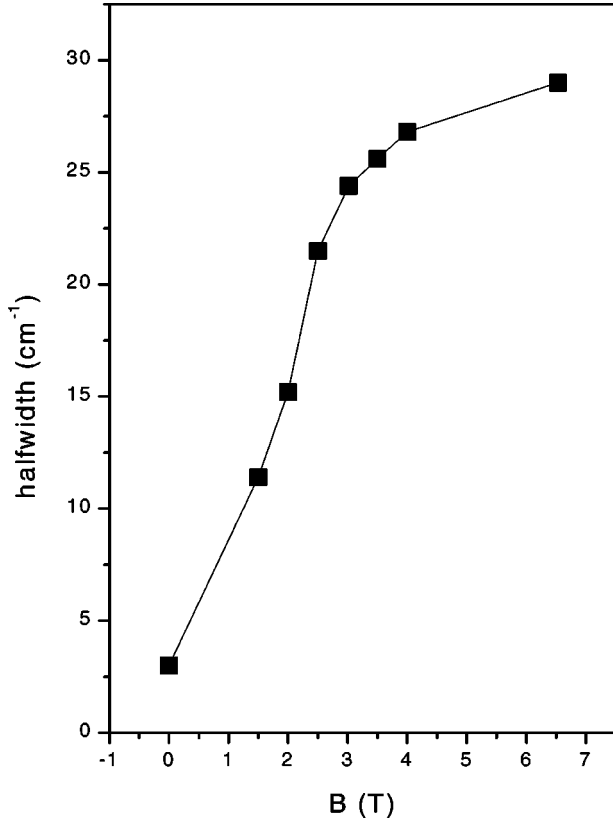


FIG. 7. The FWHM of the spin-flip line versus B . Faraday geometry, sample C, $E_{exc}=2.495$ eV, $T=1.7$ K. The solid line is a guide to the eye.

tribute this line to the Raman transition between the ground and the first excited state of antiferromagnetically coupled nearest neighbor Mn ions, namely, to the $(S=S_1+S_2=0, m=0) \rightarrow (S=1, m=0)$ transition, shown in the inset to Fig. 8. The energy levels of the pair are²⁵

$$E = -J_{NN} \left(S(S+1) - \frac{35}{2} \right) - g_{Mn} \mu_B m B, \quad (5)$$

where $S=0, 1, \dots, 5$ and $m=S, S-1, \dots, -S$. From the Raman shift of this line one can get the value of the antiferromagnetic exchange constant J_{NN} of nearest neighbor Mn pairs.

Note that the observed Raman line is actually a doublet with $\Delta\nu=3$ cm⁻¹ separation between its components. The doublet structure may be due to the presence of strain in the structure.²⁶ From the center position of the doublet we get $J_{NN} = -12.25$ K which is close to the value -12.2 K for bulk ZnSeMn known from magnetization measurements.²⁷ In Ref. 16 a value -12.8 K was found for ZnCdMnSe/ZnSe quantum wells from Raman scattering and no structure of the peak was observed. We have also detected a weaker and broader Raman line at ~ 30 cm⁻¹. It can be associated with the transition from the $S=1$ to $S=2$ level with energy equal to $4J_{NN}$. As might be expected, when the temperature increased the intensity of the line at $2J_{NN}$ decreased more strongly than that at $4J_{NN}$.

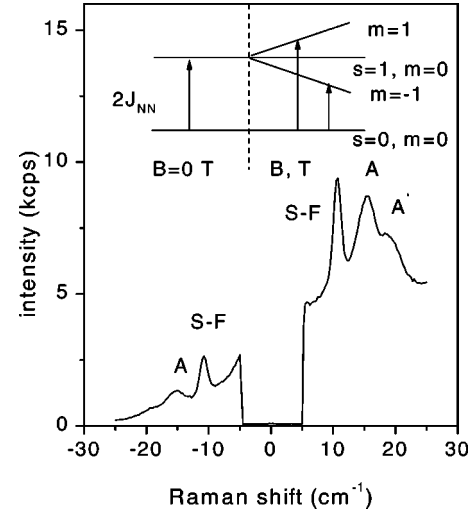


FIG. 8. Raman spin-flip transitions due to antiferromagnetically coupled nearest neighbor Mn^{2+} pairs (lines A and A'). Faraday geometry, sample A2 (five CdSe insertions), $B=0$ T, $E_{exc}=2.54$ eV, $T=10$ K. The scheme of transitions is shown in the inset. S-F line is due to a spin-flip transition associated with the donor-bound magnetic polaron.

Let us note that due to the selection rules the $2J_{NN}$ line in the backscattering Faraday configuration should be observed only in parallel circular polarization. However, we could observe it in the crossed circular polarization. On the other hand, Raman lines related to $(S=0, m=0) \rightarrow (S=1, m=\pm 1)$ transitions, which are forbidden in the Faraday configuration, were indeed not observed in the whole range of magnetic fields.

D. Multiple spin flips within Zeeman split Mn^{2+} ground state

Under resonant excitation in the Voigt backscattering geometry we observed at $B=6.5$ T and $T \sim 5$ K up to 10 equally spaced Raman lines due to multiple spin flips within a Zeeman split Mn^{2+} ground state. These lines are shown in Fig. 9 for the sample C. The Raman shift was linear in B : $E_n = ng\mu_B B$ with $g = 1.93 \pm 0.25$. The lines with odd n 's were more pronounced in crossed linear polarization $\sigma\pi$ and those with even n 's in parallel polarization $\sigma\sigma$, where π is parallel to \mathbf{B} and to the sample plane. The total intensity of the line (the sum for both polarizations) decreased exponentially as its number n increased, as is shown in Fig. 10. The appearance of a large number of lines with $n > 5$ in the Voigt geometry was first observed for CdMnTe/CdMgTe quantum wells,¹⁵ and can be explained in the framework of a theory developed in Ref. 15.

When a localized exciton is excited, an exchange field B_{exch} directed along z is produced by the heavy hole (see inset to Fig. 9). B_{exch} is directed along z because due to strong magnetic anisotropy of the valence band the heavy hole in the Voigt geometry has only $J_z = \pm 3/2$ components, $J_x = J_y = 0$. Thus B_{exch} is perpendicular to the external field B_{ext} that in the Voigt geometry is parallel to x . The effective magnetic field $B_{eff} = B_{exch} + B_{ext}$ changes its direction and the total angular momentum \vec{I} of all Mn^{2+} ions is precessing

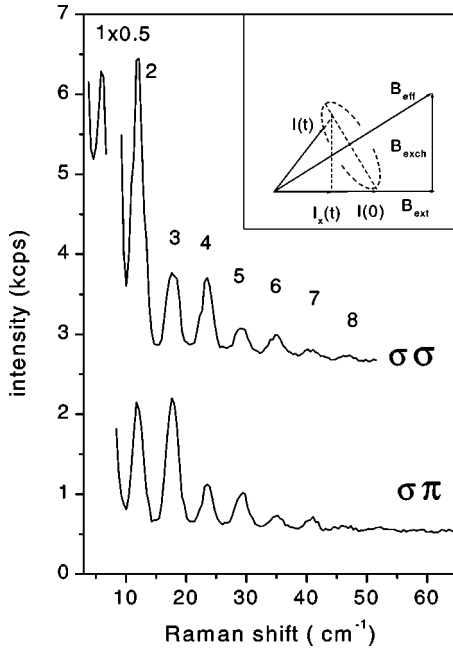


FIG. 9. Multiple spin flips within a Zeeman split Mn^{2+} ground state. Voigt geometry, sample C, $B=6.46$ T, $E_{\text{exc}}=2.54$ eV, $T=5$ K. The inset shows precession of the moment \vec{I} of all Mn^{2+} ions around the effective magnetic field (see text).

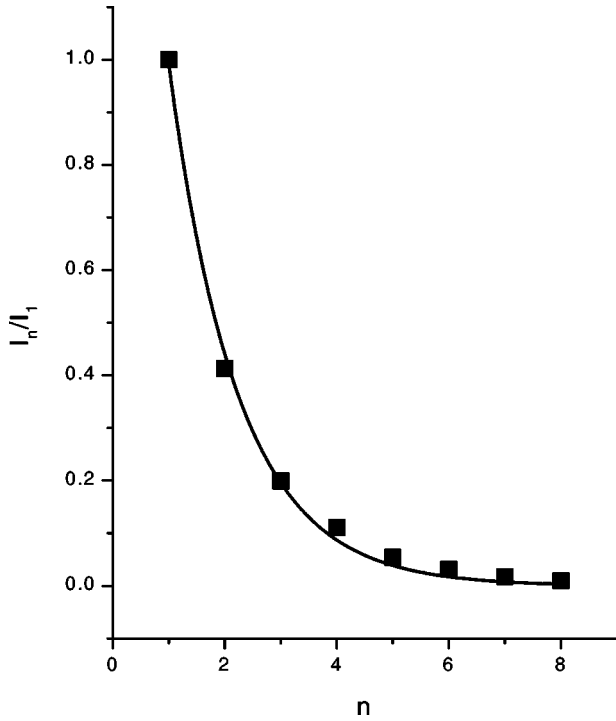


FIG. 10. Intensity of multiple Raman lines as a function of number n . Voigt geometry, sample C, $B=6.46$ T, $E_{\text{exc}}=2.54$ eV, $T=5$ K. Note that the line intensity is the sum of $\sigma\pi$ and $\sigma\sigma$ polarizations. The solid line is a fit to the function $\exp[(x-1)/1.23]$.

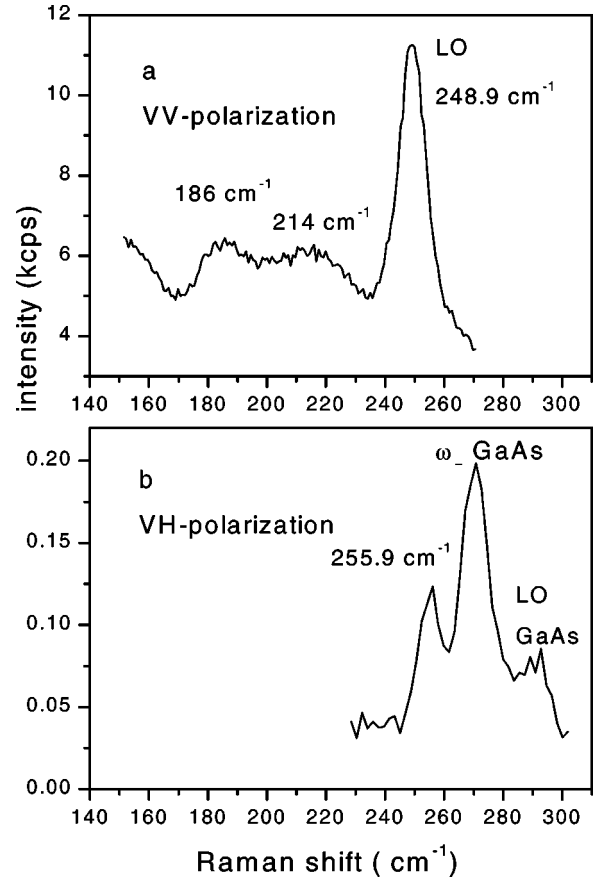


FIG. 11. Raman spectra of optical phonons. Sample C, $B=0$ T, $T=5$ K. (a) Resonance excitation, $E_{\text{exc}}=2.495$ eV; (b) off-resonance excitation $E_{\text{exc}}=2.41$ eV.

around B_{eff} . The component I_x of \vec{I} is no longer conserved and the energy of the Raman line can be an integer number n of the energy value corresponding to a single spin flip.

E. Raman scattering by optical phonons

Phonon Raman spectra were studied under resonance and off-resonance excitation. They are shown for the sample C in Fig. 11. Under resonance, Fig. 11(a), the most prominent peak is due to the averaged scattering of the LO phonons in CdZnSe islands.⁶ This peak is strongest under the outgoing resonance condition (higher order peaks of this phonon can also be observed). From the peak frequency the averaged concentration of Cd can be estimated. However, the strain in the islands and confinement effects can influence the results. In Ref. 6 for structures without Mn we estimated the average Cd concentration in the islands as 0.2, not taking into account the strain and the confinement. The compressive strain in the “well” layer of sample C due to lattice mismatch can be estimated as $\varepsilon_{\perp} = -0.0137$ (in the framework of the effective lattice constant model of Ref. 13). The strain for the barrier can be ignored. Such strain in the “well” layer could result in the shift of LO (TO) phonon lines to higher frequency by $3\text{--}4 \text{ cm}^{-1}$. The confinement in the islands could produce a shift in the opposite direction. Thus, the strain and confinement shifts would compensate each other to some extent.

There are two weak partly overlapping peaks on the low energy side of the LO peak at $\sim 186 \text{ cm}^{-1}$ and $\sim 214 \text{ cm}^{-1}$. They are not so sensitive to the resonance condition as is the LO peak and a little bit away from the resonance their relative intensities increase in comparison with the main LO peak. These two peaks with slightly varying frequencies and possibly a peak in between at 205 cm^{-1} were also observed in other samples. We attribute the peak around 214 cm^{-1} to the so called ‘‘impurity’’ mode of Cd in ZnSe.²⁸ The very weak peak around 205 cm^{-1} is the forbidden TO phonon. The nature of the peak at 186 cm^{-1} is at present unclear. This peak is clearly seen in all samples with Mn but we cannot associate it with phonons in $\text{Zn}_{1-x}\text{Mn}_x\text{Se}$,²⁹ or CdZnMnSe for reasonable concentration of the constituents.

Under the off-resonance condition, Fig. 11(b), the main peak is observed in the allowed configuration $z(xy)\bar{z}$ and its frequency corresponds to the ZnSe LO phonon. Thus this peak is related to scattering from the ZnSe layers.

IV. CONCLUSION

In conclusion, we have studied luminescence and Raman scattering in diluted magnetic structures CdSe(Mn)/ZnSe(Mn) with nominally two monolayer depositions of CdSe. The system consists of quasi-quantum CdZnSe disks in a ZnSe matrix. Mn^{2+} ions were present either in the disks or in the barriers. Luminescence observed in these samples is due to heavy hole excitons localized in the quantum disks. These excitons are also intermediate states in a number of Raman transitions by both magnetic excitations and optical phonons. The effects of strong $s,p-d$ exchange interaction of the band carriers and donor-bound electrons from the CdSe monolayers with the Mn^{2+} ions were observed in luminescence and resonance spin-flip Raman scattering, respectively.

Bound magnetic polaron formation was revealed in the spin-flip scattering at zero magnetic fields. The antiferromag-

netic exchange constant of nearest neighbor Mn^{2+} ions was obtained from the $S=0$ to $S=1$ Raman transition of Mn^{2+} nearest neighbor pairs. Collective multiple Raman scattering of paramagnetic resonance within the Zeeman split ground state of Mn^{2+} ions was observed in the Voigt configuration under resonant excitation.

It is worth noting that polarization selection rules for Raman scattering on magnetic excitations were not obeyed for the samples studied in this work. Indeed, we have observed spin-flip Raman scattering of donor-bound electrons that is forbidden in the backscattering Faraday geometry. The scattering for antiferromagnetically coupled pairs ($S=0, m=0$) $\rightarrow (S=1, m=0)$, should be seen for parallel circular polarization $\sigma_+\sigma_+$ or $\sigma_-\sigma_-$, as has already been mentioned. However, we observed it in crossed polarization.

There may be different reasons for violation of the polarization selection rules: for instance, strong localization in quantum disks of the excitons, which are intermediate states in the Raman processes, and sharp resonance conditions. Anisotropic exchange interactions may also play a role. The matter of polarization selection rules needs further study.

Raman scattering from optical phonons was studied under both resonance and off-resonance conditions with excitons localized at the CdZnSe islands, and revealed LO phonons from the averaged quantum island distribution or LO phonons from the barriers, respectively.

ACKNOWLEDGMENTS

The authors are very thankful to E. L. Ivchenko and K. V. Kavokin for fruitful discussions. This work was supported by the Russian Funds for Basic Research Grants No. 00-02-16997 and No. 99-02-18298, Volkswagen Stiftung, INTAS Grant No. 97-31907, and Grant No. 2000-1T (Russia-Ukraine) of the Program ‘‘Physics of Solid State Nanostructures.’’ S.V.I. and A.A.T. acknowledge support from the Royal Swedish Academy of Sciences.

*Email address: reshina@dnm.ioffe.rssi.ru

¹S.V. Ivanov, A.A. Toropov, S.V. Sorokin, T.V. Shubina, I.V. Sedova, A.A. Sitnikova, P.S. Kop’ev, Zh.I. Alferov, H.-J. Lugauer, G. Reuscher, M. Keim, F. Fischer, A. Waag, and G. Landwehr, *Appl. Phys. Lett.* **74**, 498 (1999).

²S.V. Ivanov, A.A. Toropov, S.V. Sorokin, T.V. Shubina, I.V. Sedova, P.S. Kop’ev, Zh.I. Alferov, A. Waag, H.-J. Lugauer, G. Reuscher, M. Keim, F.F. Fisher, and G. Landwehr, *Fiz. Tekh. Poluprovodn.* **33**, 1115 (1999) [*Semiconductors* **33**, 1016 (1999)].

³N. Peranio, A. Rosenauer, D. Gerthsen, S.V. Sorokin, I.V. Sedova, and S.V. Ivanov, *Phys. Rev. B* **61**, 16 015 (2000).

⁴D. Litvinov, A. Rosenauer, D. Gerthsen, and N.N. Ledentsov, *Phys. Rev. B* **61**, 16 819 (2000).

⁵T. Kümmell, R. Weigand, G. Bacher, A. Forchel, K. Leonardi, D. Hommel, and H. Selke, *Appl. Phys. Lett.* **73**, 3105 (1998).

⁶I.I. Reshina, A.A. Toropov, S.V. Ivanov, D.N. Mirlin, M. Keim, A. Waag, and G. Landwehr, *Solid State Commun.* **112**, 351 (1999).

⁷F. Gindele, K. Hild, W. Langbein, and U. Woggon, *Phys. Rev. B*

60, R2157 (1999).

⁸A. Kaschner, M. Strassburg, A. Hoffmann, C. Thomsen, M. Bartels, K. Lischka, and D. Schikora, *Appl. Phys. Lett.* **76**, 2662 (2000).

⁹I. Yamakawa, S.S. Sorokin, A.A. Toropov, S.V. Ivanov, and A. Nakamura, *Jpn. J. Appl. Phys., Part 2* **39**, L851 (2000).

¹⁰J.K. Furdyna, *J. Appl. Phys.* **64**, R29 (1989).

¹¹R. Fiederling, M. Keim, G. Reuscher, W. Ossau, G. Schmidt, A. Waag, and L.W. Molenkamp, *Nature (London)* **402**, 787 (1999).

¹²H. Kamada, H. Gotoh, H. Ando, J. Temmyo, and T. Tamamura, *Phys. Rev. B* **60**, 5791 (1999).

¹³E.-K. Suh, D.U. Bartholomew, A.K. Ramdas, S. Rodriguez, S. Venugopalan, L.A. Kolodzievski, and R.L. Gunshor, *Phys. Rev. B* **36**, 4316 (1987).

¹⁴M.P. Halsall, S.V. Railson, D. Wolverson, J.J. Davies, B. Lunn, and D.E. Ashenford, *Phys. Rev. B* **50**, 11 755 (1994).

¹⁵J. Stühler, G. Schaack, M. Dahl, A. Waag, G. Landwehr, K.V. Kavokin, and I.A. Merkulov, *Phys. Rev. Lett.* **74**, 2567 (1995).

¹⁶J. Puls and F. Henneberger, *J. Cryst. Growth* **214/215**, 432 (2000).

- ¹⁷The effect of luminescence band broadening under magnetic field was not observed under ultraviolet excitation and needs further investigation.
- ¹⁸R.W. Martin, R.J. Nicholas, G.J. Rees, S.K. Haywood, N.J. Mason, and P.J. Walker, *Phys. Rev. B* **42**, 9237 (1990).
- ¹⁹P. Peyla, A. Wasiela, Y. Merle d'Aubigné, D.E. Ashenford, and B. Lunn, *Phys. Rev. B* **47**, 3783 (1993).
- ²⁰D.L. Peterson, D.U. Bartholomew, U. Debska, A.K. Ramdas, and S. Rodriguez, *Phys. Rev. B* **32**, 323 (1985).
- ²¹M. Hirsch, R. Meyer, and A. Waag, *Phys. Rev. B* **48**, 5217 (1993).
- ²²I.A. Merkulov, D.R. Yakovlev, A. Keller, W. Ossau, J. Geurts, A. Waag, G. Landwehr, G. Karczewski, T. Wojtowicz, and J. Kossut, *Phys. Rev. Lett.* **83**, 1431 (1999).
- ²³M. Nawrocki, R. Planel, G. Fishman, and R. Galazka, *Phys. Rev. Lett.* **46**, 735 (1981).
- ²⁴T. Dietl and J. Spałek, *Phys. Rev. B* **28**, 1548 (1983).
- ²⁵D.U. Bartholomew, E.-K. Suh, S. Rodriguez, A.K. Ramdas, and R.L. Aggarwal, *Solid State Commun.* **62**, 235 (1987).
- ²⁶The line of analogous origin studied in bulk CdMnS (Ref. 25) was also found to be a doublet with $\Delta\nu=1.6\text{ cm}^{-1}$. The doublet structure was related to the existence in the wurtzite structure of CdMnS of two types of nearest neighbor pairs having slightly different values of J_{NN} .
- ²⁷D. Heiman, in *Proceedings of the 12th International Conference on High Magnetic Fields in the Physics of Semiconductors*, edited by G. Landwehr and W. Ossau (World Scientific, Singapore, 1997), Vol. II, p. 847.
- ²⁸R.G. Alonso, E.-K. Suh, A.K. Ramdas, N. Samarth, H. Luo, and J.K. Furdyna, *Phys. Rev. B* **40**, 3720 (1989).
- ²⁹T.R. Yang, C.C. Lu, W.C. Chou, Z.C. Feng, and S.J. Chua, *Phys. Rev. B* **60**, 16 058 (1999).